Proceedings of ISINN-29, JINR, E3-2023-58, Dubna, 2023, p.306 – 320

^{236s}Np isomer yields in ^{237}Np(n,2n) and ^{238}U(p,3n) reactions

Vladimir Maslov[1]

220025, Minsk, Byelorussia

Modeling $r(E_n)$, ratio of the yields of short-lived (1^-) and long-lived (6^-) of ^{237}Np(*n*,2*n*) reaction from threshold energy up to 20 MeV allowed to infer also the yield of the short-lived state ^{236s}Np in ^{238}U(*p*,3*n*) reaction. The different initial spin populations is probed in (*p*,3*n*) and (*n*,2*n*) reactions. The consistent description of the data base on cross sections ^{237}Np(*n*,*F*), ^{237}Np(*n*,2*n*)^{236s}Np and ^{238}U(*p*,*F*), ^{238}U(*p*,*n*) and ^{238}U(*p*,3*n*)^{236s}Np is achieved. The branching ratio $r(E_n)$ obtained by modeling the residual nuclide ^{236}Np levels. Excited levels of ^{236}Np are modeled using predicted Gallher-Moshkowski doublets. The branching ratios $r(E_n)$ and $r(E_p)$ are defined by the ratio of the populations of the two lowest states, isomer ^{236s}Np, with spin *J*= 1 and ground state ^{236l}Np with spin *J*= 6. The $r(E_n)$ and $r(E_p)$ have similar shapes in case of (*n*,2*n*) and (*p*,3*n*) reactions, which is due to some internal compensation of differing angular momentum and excitation energy distributions of ^{236}Np yields. The populations of ^{236s}Np and ^{236l}Np states defined by the γ-decay of the excited states of ^{236}Np in the continuum. The exclusive spectra of (*n,xnf*) and (*n,2n*)^{1,2} and (*p,xnf*) and (*p*,3*n*)^{1,2,3} influence $r(E_n)$ and $r(E_p)$ at higher energies and prompt fission neutron spectra.

Neptunium-237 is a major constituent of the spent nuclear fuel. Main chains for its production are neutron captures in ^{235}U and (*n, 2n*) reactions in ^{238}U, namely, ^{235}U(*n, γ*) ^{236}U(*n*, γ) ^{237}U(β$^-$)^{237}Np and ^{238}U(*n,2n*) ^{237}U(β$^-$)^{237}Np. The transmutation of the ^{237}Np in thermal power reactors is affected by the neutron capture cross sections of the reaction chain ^{237}Np(n,γ) ^{238}Np(β$^-$)^{238}Pu(*n*,γ) ^{239}Pu. The yield of the ^{236s}Np short-lived isomer happens via reaction chain ^{237}Np(*n*,2*n*) ^{236s}Np(β$^-$) [1−4].

The reaction chain ^{237}Np(*n*,2*n*)^{236s}Np(β$^-$)^{236}Pu(α)^{232}U is one of the major sources of the accumulation of ^{232}U in the irradiated reactor fuel. The half-life of ^{236s}Np $T^s_{1/2} = 22.5h$, the long-lived state, emerging in the reaction ^{237}Np(*n*,2*n*) ^{236l}Np ($T^l_{1/2} = 1.55\times10^5 y$) has a large thermal fission cross section, which may strongly influence the nuclear core reactivity [5]. Modeling $r(E_n)$, ratio of the yields of short-lived (1^-) and long-lived (6^-) of ^{237}Np(*n*,2*n*) reaction from threshold energy up to 20 MeV allowed to infer the yield of the short-lived state ^{236s}Np in ^{238}U(*p*,3*n*) reaction. The $r(E_n)$ and $r(E_p)$ are susceptible to the influence of differing initial spin populations probed in (*p*,3*n*) and (*n*,2*n*) reactions. The exclusive spectra of (*n,xnf*) , (*n*,2*n*)^{1,2} and (*p,xnf*) , (*p*,3*n*)^{1,2,3} influence $r(E_n)$ and $r(E_p)$ at higher energies and prompt fission neutron spectra [6−8]. They are used to define the exclusive spectra of (*n*,2*n*)^{1,2} reaction. These latter spectra define populations of ^{236}Np states.

The yield of short-lived 1^- state in ^{237}Np(*n*,2*n*) ^{236s}Np measured in the vicinity of the threshold [9] and around 14 MeV [10−15]. The ratio of yields of short- and long-lived states measured at ~14 MeV [16] allows to check the compatibility of measured data on ^{237}Np(*n*,2*n*)^{236s}Np reaction with the calculated cross sections of ^{237}Np(*n*,2*n*) and ^{237}Np(*n*,*F*).

[1]mvmmvm2386@yandex.ru

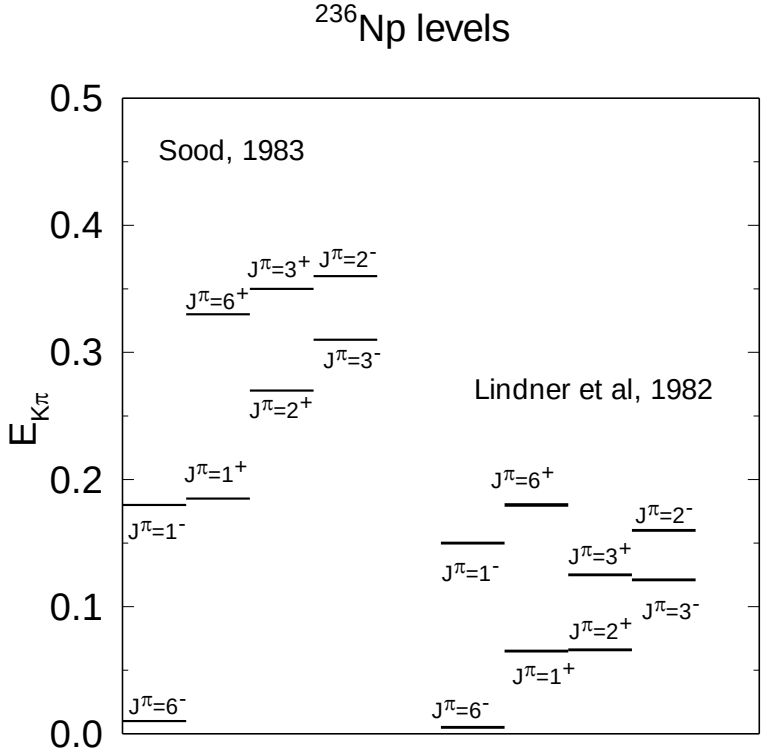

Fig. 1 Levels of ^{236}Np.

$$r(E_n) = \sigma^{l}_{\mathrm{n2n}}(E_n)/\sigma^{s}_{\mathrm{n2n}}(E_n), \qquad (1)$$

That means consistent description of the data base on fission and ^{237}Np(n,2n)^{236s}Np might be challenged at E_n~14 MeV, while at lower and higher values of E_n the $r(E_n)$ might be predicted. The branching ratio $r(E_n)$ is rather sensitive to the residual nuclide ^{236}Np levels. Excited levels of ^{236}Np are modeled using predicted Gallher-Moshkowski doublets by Sood [17] and Lindner et al. [18]. Modeling of the ratio of the yields of short-lived (1^-) and long-lived (6^-) from threshold energy of (n,2n) reaction up to 20 MeV, allows to infer the yield of the short-lived state ^{236s}Np as

$$\sigma^{s}_{n2n}(E_n) = \sigma_{n2n}(E_n)/(1+r(E_n)). \qquad (2)$$

It provides a description of ^{237}Np(n,2n) ^{236s}Np data around E_n~14 MeV [10−15] and data from ^{237}Np (n,2n) reaction threshold up to E_n ~10 MeV [9].

Cross sections of (n,2n) and (n,3n) reactions are obtained with the statistical model calculations with account of pre-equilibrium neutron emission. Pre-equilibrium neutron emission contribution fixed according to consistent description of (n, F) and (n,xn) reaction data [3]. Myers et al. [16] measured the isomer branching ratio $r(E_n) = \sigma^{l}_{n2n}(E_n)/\sigma^{s}_{n2n}(E_n)$ with neutrons of the thermonuclear bomb-shot for the average beam energy of ~14 MeV. In the report [11] the isomer ratio $r(E_\gamma) = \sigma^{l}_{\gamma n}(E_n)/\sigma^{s}_{\gamma n}(E_n)$ of ~0.41 for ^{237}Np(γ,n) reaction was mentioned

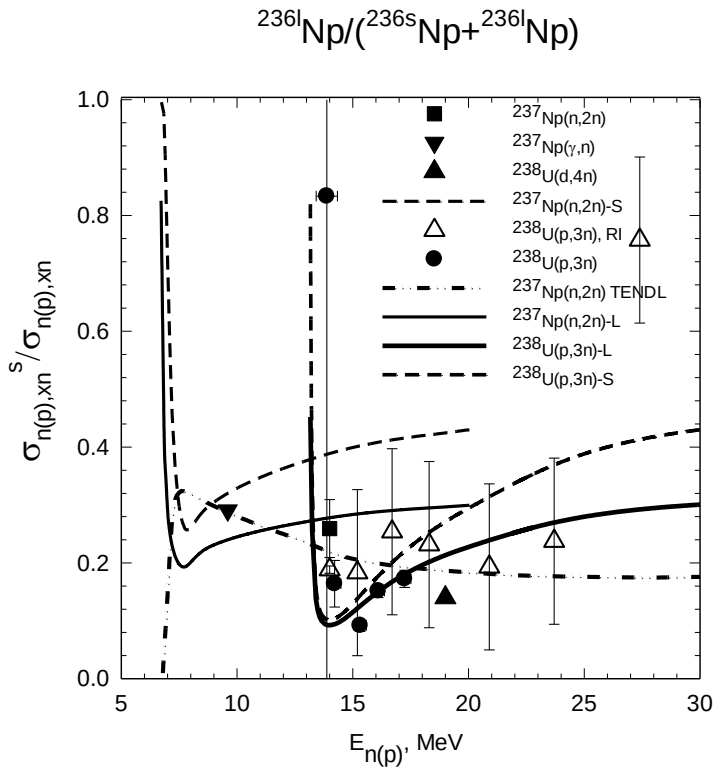

Fig. 2 Relative yield of long-lived (6^-) ^{236l}Np state in ^{237}Np(n,2n) and ^{238}U(p,3n) reactions; ■– [9]; ▼– [11];▲– [19]; ●– [49]; Δ– [48].

for the excitation energy of ~9.6 MeV. That presents the evidence of the decrease of $r(E_n)$ with the increase of the incident neutron energy E_n, if not the possible influence of the entrance channel on the initial spin population of ^{236}Np residual/excited nuclide. That conclusion is supported also by the data on the isomer branching ratio for the reaction ^{238}U(d,4n) for E_d~21 MeV [19]. In [19] it was found that the states of the residual nuclide ^{236s}Np with J= 1 are ~7 times more populated than the states ^{236l}Np with spin J=6. The modeling of the $r(E_n)$ for the ^{237}Np(n,2n) gives complex behavior, than just fitting [20], the trend of $r(E_{n,\gamma,d})$ measured values.

The branching ratio $r(E_n)$ is defined by the ratio of the populations of the two lowest states of ^{236s}Np, with spin J= 1 and ^{236l}Np, with spin J= 6. These populations defined by the γ-decay of the continuum excited states of ^{236}Np. For (n,γ) reaction the γ-decay was modeled in [21]. That approach could be applied in case of ^{237}Np(n,2n) or ^{238}U(p,3n) reactions probing the different initial spin populations for neutron capture, (n,2n) and (p,3n) reactions.

The γ-decay of the excited nucleus described by the following kinetic equation [21]

$$\frac{\partial \omega_k(U,J^\pi,t)}{\partial t} = \sum_{J'\pi'} \int_0^{U_g} \omega_{k-1}(U',J^\pi',t) \frac{\Gamma_\gamma(U',J^\pi',U,J^\pi)}{\Gamma(U',J^\pi')} dt - \omega_k(U,J^\pi,t) \frac{\Gamma_\gamma(U,J^\pi)}{\Gamma(U,J^\pi)}, \quad (3)$$

here $\omega_k(U,J^\pi,t)$ is the population of the state J^π at excitation U at time t, after emission of k γ-quanta; $\Gamma_\gamma(U',J^\pi',U,J^\pi)$ is the partial width of γ-decay from the (U',J^π') to the state (U,J^π),

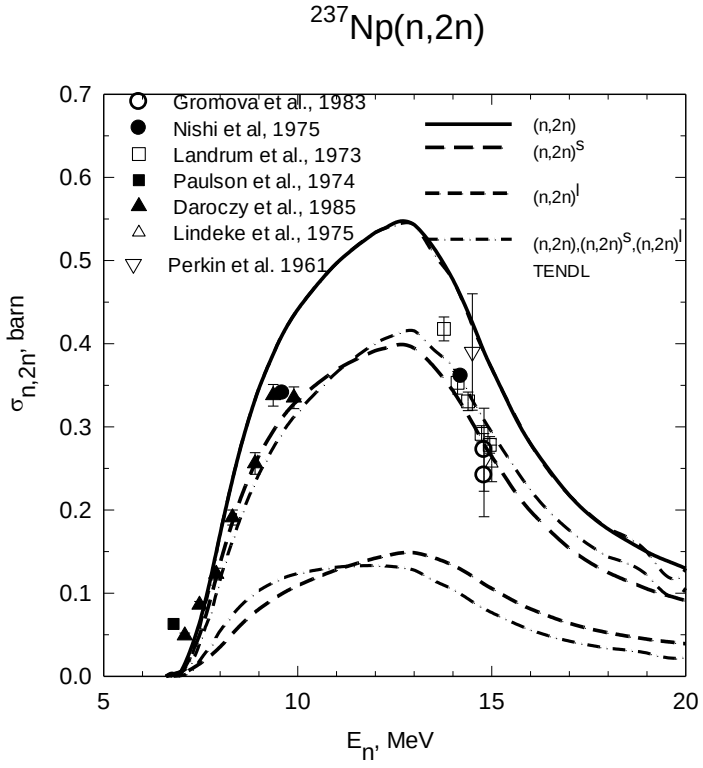

Fig. 3 Cross sections of ^{237}Np(*n*,2*n*), ^{237}Np(*n*,2*n*)^{236s}Np and ^{237}Np(*n*,2*n*)^{236l}Np reaction.

while $\Gamma(U,J^\pi)$ is the total decay width of the state (U,J^π). For any state (U,J^π) with the excitation energy $0 \le U \le U_g$, the initial population is

$$\omega_k(U,J^\pi,t=0) = \delta_{ko}\omega_0(U,J^\pi). \qquad (4)$$

The equation (4) means that in the initial state of (*n*,2*n*) or (*p*,3*n*) reactions we deal with the ensemble of states (U,J^π). Integrating the Eq. (3) over *t*, one gets the population $W(U,J^\pi)$ of the state (U,J^π) after emission of *k* γ-quanta:

$$\omega_k(U,J^\pi,\infty) - \omega_k(U,J^\pi,0) = \sum_{J'\pi'}\int_U^{U_g}\frac{\Gamma_\gamma(U',J^\pi',U,J^\pi)}{\Gamma(U',J^\pi')}\int_0^\infty \omega_{k-1}(U',J^\pi',t)dtdU' -$$

$$\frac{\Gamma_\gamma(U,J^\pi)}{\Gamma(U,J^\pi)}\int_0^\infty \omega_k(U,J^\pi,t)dt. \qquad (5)$$

Denoting the population of the state (U,J^π) after emission of *k* γ-quanta as

$$W_k(U,J^\pi) = \frac{\Gamma_\gamma(U,J^\pi)}{\Gamma(U,J^\pi)}\int_0^\infty \omega_k(U,J^\pi,t)dt\,, \qquad (6)$$

and taking into account the condition that $\omega_k(U, J^\pi, \infty) = 0$ for any state, belonging to ensemble (U, J^π), Eq. (5) could be rewritten [21, 22] as

$$W_k(U, J^\pi) = \sum_{J'\pi'} \int_U^{U_g} \frac{\Gamma_\gamma(U', J^\pi', U, J^\pi)}{\Gamma(U', J^\pi')} W_{k-1}(U', J^\pi') dU' + \omega_k(U, J^\pi, 0). \quad (7)$$

The population of any state (U, J^π) after emission of any number of γ-quanta defined as

$$W(U, J^\pi) = \sum_k W_k(U, J^\pi), \quad (8)$$

then from Eq. (6) one easily gets [21, 22]

$$W(U, J^\pi) = \sum_{J'\pi'} \int_U^{U_g} \frac{\Gamma_\gamma(U', J^\pi', U, J^\pi)}{\Gamma(U', J^\pi')} W(U', J^\pi') dU' + W_0(U, J^\pi). \quad (9)$$

The integral equation (9) in the code STAPRE [23] solved as a system of linear equations, the integration range (U, U_g) binned, in the assumption that there are no γ-transitions inside the narrow energy bins.

The isomer branching ratio depends mostly on the low-lying levels scheme and relevant γ-transitions probabilities. The latter data are missing for the ^{236}Np nuclide. As regards the low-lying levels of odd-odd nuclides like ^{236}Np, extensive experimental data are available only for ^{238}Np, ^{242}Am, ^{244}Am and ^{250}Bk [24]. It was established for the ^{236l}Np [19, 24] that the decay of ^{236l}Np(β$^-$) ^{236}Pu yields $J^\pi = 6^+$ states, while in e-capture the yield of $J^\pi = 6^+$ state of ^{236}U is observed. That is a strong argument that the long-lived state might be $J^\pi = 6^-$. It was established for the ^{236s}Np [18, 25–28], that the decay ^{236s}Np(β$^-$)^{236}Pu yields $J^\pi = 0^+, 2^+$ states, while in e-capture the yield of $J^\pi = 0^+, 2^+, 2^-$ states of ^{236}U is observed. That is a strong argument, that for the short-lived state $J^\pi = 1$, while the parity of the low-spin short-lived state is still uncertain. With these arguments one may stay assured that the spins of the two low-lying states of ^{236}Np are fixed. What are the energies of the ^{236s}Np and ^{236l}Np states is uncertain also. There is no experimental data about the other low-lying levels of ^{236}Np, with the exception of $J^\pi = 3^-$, which was observed in [28] when investigating the enhanced α-decay of ^{240}Am.

Modeling of low-lying levels of in [17, 18] is accomplished based on the assumption that ground and first few excited states are of two-quasi-particle nature. For actinides with quadrupole deformations the superposition principle is usually adopted, the band-head energies of the doubly-odd nucleus are generated by adding to the each unpaired configuration (Ω_p, Ω_n), as observed in the isotopic/isotonic nucleus, the rotational energy contribution and residual *n*–*p* interaction energy contribution. The angular momenta of neutron and proton quasi-particles could be parallel or anti-parallel. In the independent quasi-particle model the two-quasi-particle states, $K^+ = |K_n + K_p|$ and $K^- = |K_n - K_p|$, are degenerate. Gallaher-Moshkowski doublets [17, 18] appear because of *n*–*p* residual interaction. Figure 1 (left) shows the predicted in [17] band-head energies for the two-quasi-particle states expected up to ~400 keV in the odd-odd nuclide

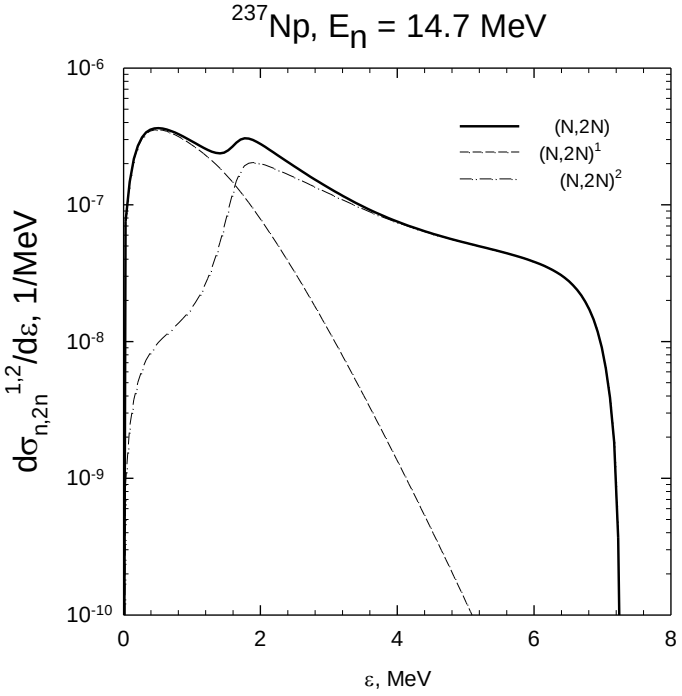

Fig. 4 Exclusive (*n*, 2*n*) neutron spectra of ^{237}Np+n for incident neutron energy 14.7 MeV.

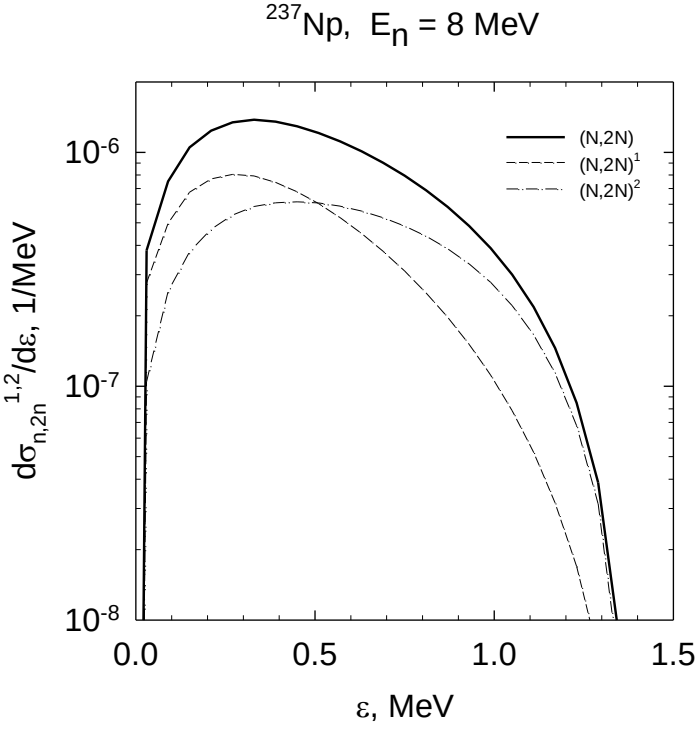

Fig. 5 Exclusive (*n*, 2*n*) neutron spectra of ^{237}Np+n for incident neutron energy 8 MeV.

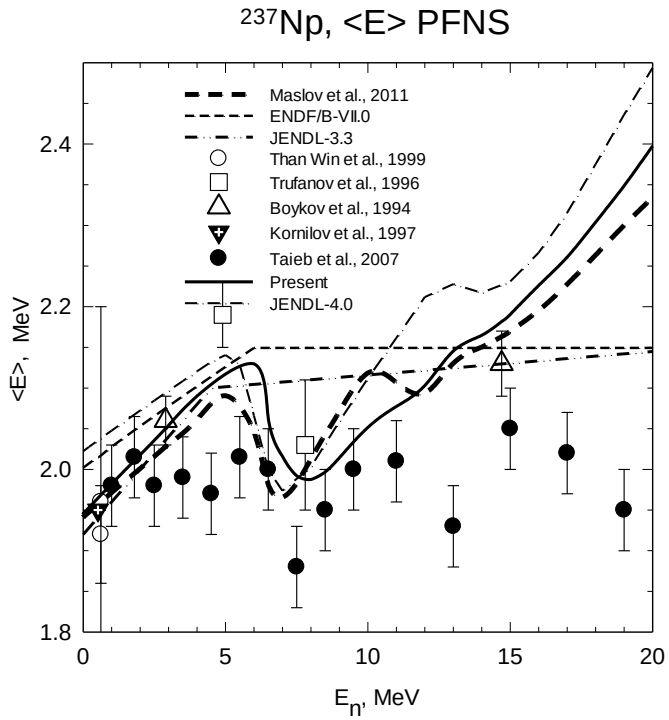

Fig. 6 Dependence of average energy of ^{237}Np(n,F) prompt fission neutrons on the E_n.

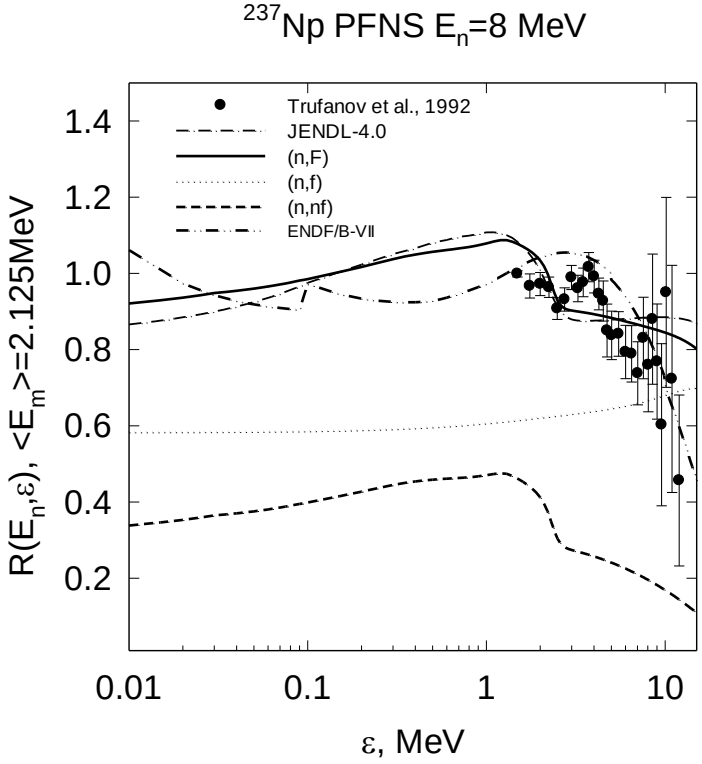

Fig. 7 Multiple-chance fission contributions to the prompt fission neutron spectrum for ^{237}Np (n, F) reaction, incident neutron energy ~8 MeV plotted as a ratio to Maxwellian with of <E>=2.125 MeV.

^{236}Np. The spectroscopic properties of two pairs of proton and neutron single particle states were derived from those experimentally observed in the isotopic (Z=93) and isotonic (N=143) odd-mass nuclei with mass (A-1). Figure 1 (right) shows levels expected up to ~250 keV of [18]. Obviously, the relative placement of LSI (low spin isomer), as well as its parity are different, though the underlying proton and neutron single particle states are similar. In short, in [17] LSI $J^{\pi}=1^{-}$ is just below $J^{\pi}=1^{+}$ counterpart, while in [18] the predicted LSI $J^{\pi}=1^{+}$ is lying much lower than the $J^{\pi}=1^{-}$ counter-part. However, the splits of LSI and HSI of [17] and [18] are quite different. For the band-heads, shown on Figure 1, the rotational bands generated as

$$E_{JK\pi}=E_{JK}+5.5\left[J(J+1)-K(K+1)\right]. \qquad (10)$$

Obviously, neither of the schema presented on Fig. 1 represents a complete set to allow the calculation of absolute yields of ^{237}Np(n,2n)^{236s}Np and ^{237}Np(n,2n)^{236l}Np reactions. However, in both cases attributed rotational bands were constructed up to ~700 keV, modeling levels with spins $J^{\pi}\le 10$, in total up to ~70 levels. It was shown in [29], that simple estimate of the number of levels in odd-odd nuclei as

$$N(U)=e^{2\Delta_0/T}(e^{U/T}-1), \qquad (11)$$

predicts up to 280 level at U~700 keV, T=0.388 MeV, $\Delta=12/A^{1/2}$, MeV. We assume that the modeled angular momentum distribution would not be much different from a real one. Since the data on the γ-transitions are missing, we assumed the simple decay scheme, i.e. only E1, E2 and M1 transitions allowed in continuum energy range. Inter-band transitions forbidden, i.e., only γ-transitions within the rotational bands are assumed to occur. This methodology pursued, the populations of the lowest doublets calculated. Then we assumed that the transition to the high-spin, long-lived ground state $J^{\pi}=6^{-}$ or low-spin, short-lived isomer state $J^{\pi}=1^{-}$ [17] or $J^{\pi}=1^{+}$ [18] defined by "minimum multi-polarity" rule. That means states with spins $J>3$ should populate the ground state $J^{\pi}=6$, while those with $J\le 3$ should feed the isomer state J^{π} =1.

Then the branching ratio obtained as the ratio of the level populations, derived from Eq. (9):

$$r(E_n)=\frac{\sum_{J>(J_l+J_s)/2}W(U,J^{\pi})}{\sum_{J\le(J_l+J_s)/2}W(U,J^{\pi})} \qquad (12)$$

Figure 2 shows the branching ratios, calculated for the level schema of [17] and [18], presented at left and right parts of Fig. 1. The level scheme of [18] appears to be compatible with the measured data for $r(E_n)=\sigma^{l}_{\mathrm{n2n}}(E_n)/\sigma^{s}_{\mathrm{n2n}}(E_n)$ at 14 MeV [16], it is adopted in [3, 32], while the branching ratio for the level scheme of [17] has a similar shape of $r(E_n)$, but higher absolute value. The measured data of [11] and [19] for ^{237}Np(γ,n) and ^{238}U(d,4n) reactions, respectively, are much different from the predicted trend. The $r(E_n)$ in JENDL-4 [30] is independent on the energy of incident neutron, which strongly contradicts present predicted shape. The branching

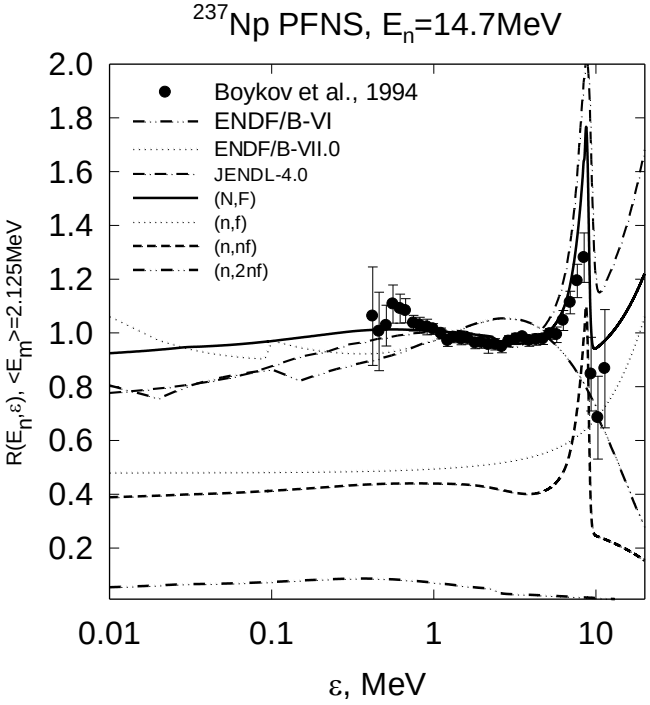

Fig. 8 Multiple-chance fission contributions to the prompt fission neutron spectrum for ^{237}Np (*n,F*) reaction, incident neutron energy 14.7 MeV plotted as a ratio to Maxwellian with average energy of $\langle E \rangle$=2.125 MeV.

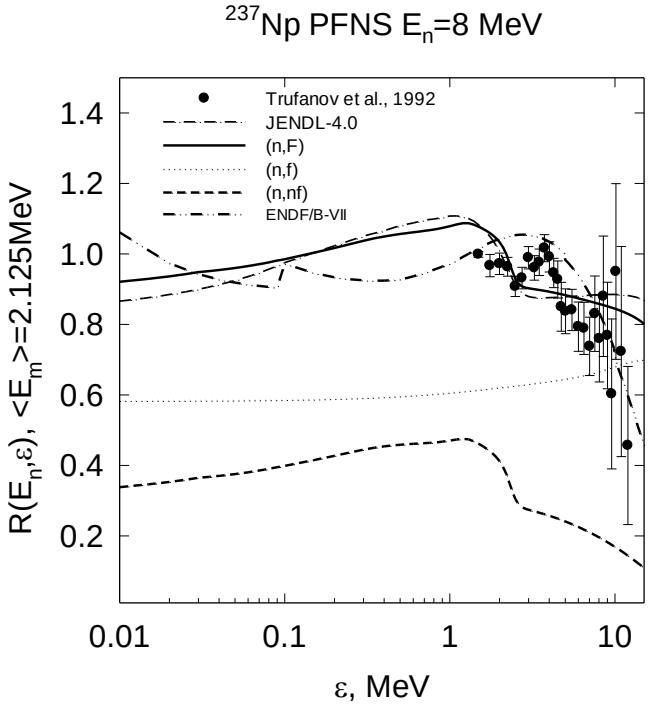

Fig. 9 Multiple-chance fission contributions to the prompt fission neutron spectrum for ^{237}Np (*n,F*) reaction, incident neutron energy 8 MeV plotted as a ratio to Maxwellian with average energy of $\langle E \rangle$= 2.125 MeV.

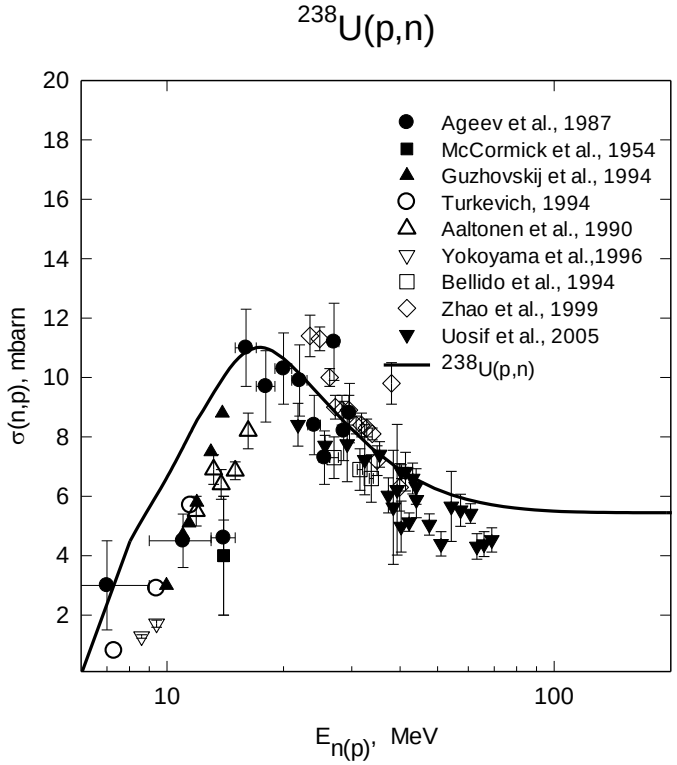

Fig. 10 Cross sections of ^{238}U(*p, n*).

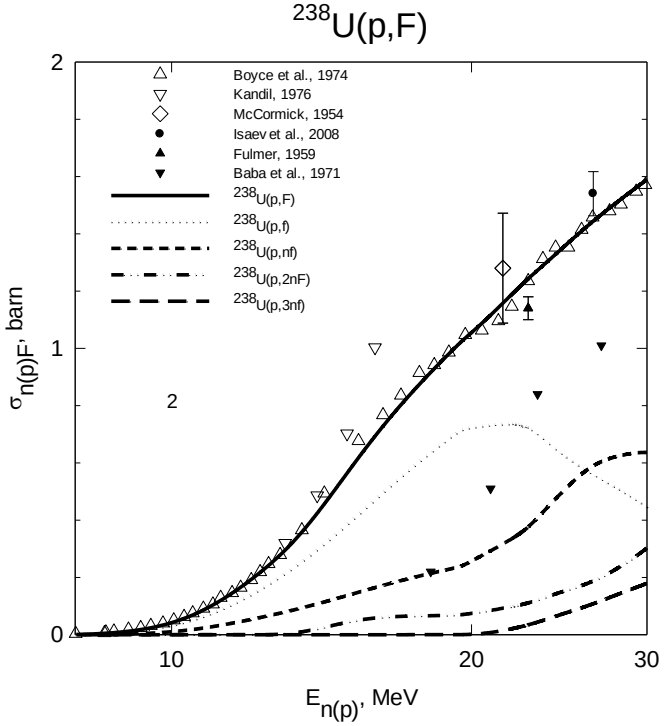

Fig, 11 Multiple-chance fission contributions to ^{238}U(*p,F*) reaction.

ratio $r(E_n)$ of ENDF/B-VIII [31] is adopted from [3, 32]. The branching ratio $r(E_n)$ used to estimate ^{237}Np(n,2n) ^{236s}Np and ^{237}Np(n,2n)^{236l}Np reaction cross sections using ^{237}Np(n,2n) reaction cross section compatible with ^{237}Np(n,F) cross section [2, 33].

Figure 3 shows ^{237}Np(n,2n), ^{237}Np(n,2n)^{236s}Np and ^{237}Np(n,2n)^{236l}Np reaction cross sections. Measured data base on ^{237}Np(n,2n)^{236s}Np [9-15] was corrected in [3] using the modern decay and cross section data standards. The decay data for the ^{236m}Np were those from [33]. Recent evaluation by E.Browne and J.K.Tuli [34], which is in Decay Radiation Data Base [35], is consistent with the former data of [33]. The half-life, estimated in [33, 34] is $T_{1/2}$= (22.5±0.04) hours. The electron-capture and β$^-$-decay branching ratios of [34] equal: I_{ec} =0.52±0.01 and $I_{\beta-}$ =0.48±0.01, respectively. In [35] $I_{ec} = I_{\beta-}$ = 0.50±0.03. The neutron flux monitor reaction were those of ^{27}Al(n,α)^{24}Na, ^{238}U(n,2n)^{238}U and ^{238}U(n,f), evaluated in [36], [37] and [38], respectively. It was possible to update measured database, except data [15]. ^{237}Np(n,2n), ^{237}Np(n,2n)^{236s}Np and ^{237}Np(n,2n)^{236l}Np reaction cross sections [3, 32] shown on Fig. 2 are adopted in [31], in [20] they adopted ^{237}Np(n,2n) cross section only. Though ^{237}Np(n,2n)^{236s}Np and ^{237}Np(n,2n)^{236l}Np reaction cross section of [20] seem to be close to those of [3, 32], the branching ratios $r(E_n)$ are very much different, since in [20] the $r(E_{n,\gamma,d})$ just reproduces trend measured values of (γ,n), (n,2n) and (d,4n) reactions.

Exclusive spectra of first neutrons, $\frac{d\sigma^1_{n2n}}{d\varepsilon}$, and $\frac{d\sigma^2_{n2n}}{d\varepsilon}$ second neutrons of (n,2n) reaction, calculated as in [39−41] are shown on Fig. 4 and Fig. 5. They define the populations of ^{236}Np nuclide states. The spectra presented normalized to 10^{-6}, since in data files [3, 32] the emitted neutron energies given in eV. The major competing reaction to ^{237}Np(n,2n) is ^{237}Np(n,xnf). Actually, x pre-fission neutrons define the shape of exclusive spectra of first neutrons, $\frac{d\sigma^1_{n2n}}{d\varepsilon}$, and $\frac{d\sigma^2_{n2n}}{d\varepsilon}$ second neutrons. They influence also the average energy of prompt fission neutrons measured in [42−46] as shown on Fig. 6, and shapes of prompt fission neutron spectra (PFNS). Figures 7 and 8 demonstrate the PFNS at E_n~14.7 MeV and E_n~8 MeV. The partial contributions of observed PFNS are sensitive to ^{237}Np(n,xnf) contributions to the observed fission cross section ^{237}Np(n,F) [3] and exclusive pre-fission neutron spectra.

Modeling the ratio $r(E_n)$ of the yields of short-lived (1$^-$) and long-lived (6$^-$) of ^{237}Np(n,2n) reaction from threshold energy up to 20 MeV allows to infer the yields of the short-lived state ^{236s}Np and long-lived state ^{236l}Np in ^{238}U(p,3n) reaction. Since entrance channel J^π populations in case of ^{238}U+p and ^{237}Np are quite different [47] as well as spin populations of (p,3n) and (n,2n) reactions, $r(E_n)$ and $r(E_p)$ would demonstrate various behavior. The consistent description of the data base on fission reaction ^{238}U(p,F) and ^{238}U(p,n) and ^{238}U(p,3n)^{236s}Np was achieved within STAPRE environment [23]. The contribution of the yield ^{238}U(p,3n)^{236s}Np to the ^{238}U(p,3n) reaction cross section is compatible with measured data on $r(E_p)$ [48] and [49]. The contribution of the yield ^{238}U(d,4n)^{236s}Np to the ^{238}U(d,4n) would have similar shape, but shifted to higher energies.

The absolute values of ^{238}U(p,3n)^{236s}Np contribution to the ^{238}U(p,3n) are obtained simultaneously with ^{238}U(p,F) and ^{238}U(p,n) cross sections. Fig. 10 shows description of ^{238}U(p,n) data [49−57] up to E_p~70 MeV with the direct neutron emission as described in [39, 40], with the exception that the (p,nX)^1 spectra are much softer than in case of ^{237}Np+n interaction.

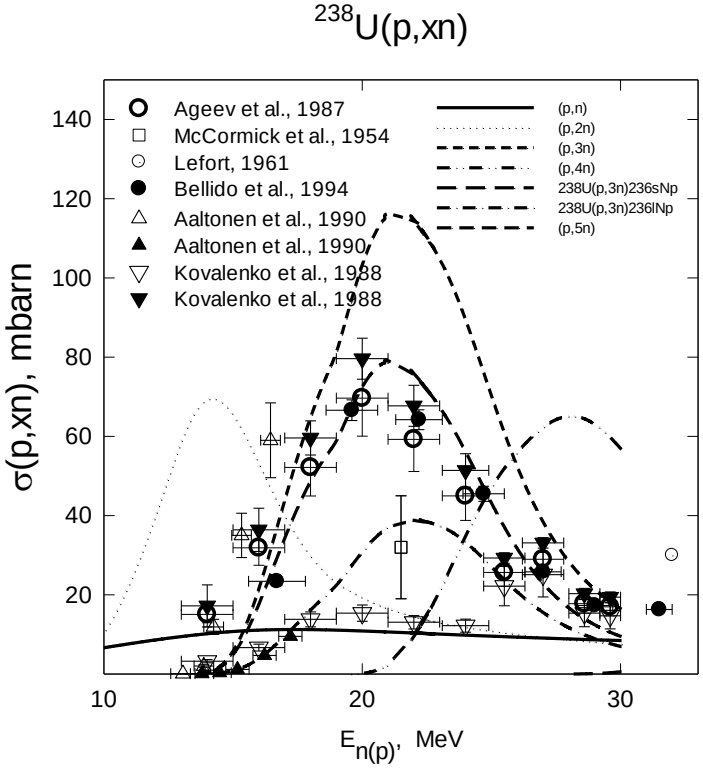

Fig. 12 Cross sections of ^{238}U(*p*,2*n*), ^{238}U (*p*,3*n*), ^{238}U (*p*,3*n*)^{236s}Np and ^{238}U (*p*,3*n*)^{236l}Np reaction. neutron spectra [39−41].

Fission reaction cross section ^{238}U(*p, F*) comprise the major part of proton absorption cross section which is defined in [47]. Modelling the (*p,nX*)[1] spectra in a way described in [39, 40] the ^{238}U(*p,F*) data could be reproduced up to 200 MeV. Figure 11 shows the fission cross section data [58−62] up to E_p~30 MeV and partial contributions of ^{238}U(*pxnf*) chances to the observed cross section of ^{238}U(*p,F*). Figure 11 shows the calculated symmetric ^{238}U(*p,xnf*)^{sym}, asymmetric ^{238}U(*p,xnf*)^{asym} and ^{238}U(*p,F*) fission cross sections. In case of the proton-induced fission reaction ^{238}U(*p,F*) the observed fission reaction cross section is calculated using the fission-barrier and level-density parameters of Np nuclei, obtained by fitting the ^{237}Np(*n,F*) fission cross section [32]. It might be anticipated that ^{238}U(*p,xnf*) reactions give the dominant contribution to the observed fission cross section [63].

Absolute values of ^{238}U (*p*,3*n*)^{236s}Np and ^{238}U (*p*,3*n*)^{236l}Np contributions to the ^{238}U(*p*,3*n*) cross section measured data are compared on Fig. 12. Data [49] are quite compatible with calculated cross sections of ^{238}U (*p*,3*n*)^{236s}Np and ^{238}U (*p*,3*n*)^{236l}Np reactions. In case of data [48] there is some discrepancy around peak crass section values.

Modeling $r(E_{n(p)})$, ratio of the yields of short-lived (1^-) ^{236s}Np and long-lived (6^-) ^{236l}Np in ^{237}Np(*n*,2*n*) reaction from threshold energy up to 20 MeV and ^{238}U(*p*,3*n*) reaction from threshold energy up to 30 MeV allowed to describe the measured yield of the short-lived state ^{236s}Np. The different initial spin populations are probed in (*p*,3*n*) and (*n*,2*n*) reactions. The consistent description of the data base on cross sections of fission ^{237}Np(*n,F*) , ^{237}Np(*n*,2*n*)^{236s}Np and ^{238}U(*p,F*), ^{238}U(*p,n*) and ^{238}U(*p*,3*n*)^{236s}Np is achieved. The branching ratio $r(E_n)$ obtained by modeling the residual nuclide ^{236}Np levels using predicted Gallher-Moshkowski doublets.

The branching ratio $r(E_n)$ is defined by the ratio of the populations of the two lowest states, isomer ^{236s}Np, with spin J= 1 and ground state ^{236l}Np with spin J= 6. The $r(E_n)$ and $r(E_p)$ have similar shapes in case of (n,2n) and (p,3n) reactions, which is due to internal compensation of differing angular momentum and excitation energy distributions of ^{236}Np yields. The populations of ^{236s}Np and ^{236l}Np states defined by the γ-decay of the excited states of ^{236}Np in the continuum. The exclusive spectra of (n,*xnf*) and (n,2n)[1,2] and (p,*xnf*) and (p,3n)[1,2,3] influence $r(E_n)$ at higher energies and prompt fission neutron spectra [64].

References

1. Ignatyuk A.V., Kornilov N.V., Maslov V.M., Atomnaya Energiya 63, 110 (1987).
2. Maslov V.M. VANT, Ser. Yad, Konst., 4, 1987, INDC(CCP)-366, p. 27, 1994 .
3. Maslov V.M., Pronyaev V.G., N.A. Tetereva, Kolesov A.M., Zolotarev K.I., Granier T., Hambsch F.-J., INDC (BLR)-21, Vienna: IAEA, 2003; https://www-nds.iaea.org/publications/ indc/indc-blr- 0021/
4. Fort E., Derrien H., Doat J.P. In: Proc. Int. Conf. Nuclear Data for Science and Technology, Antwerpen, Belgium, September 6-10, 1982, p. 673, 1983.
5. Belyaev B.N., Gromova E.A., Kovalenko S.S. et al., Atomnaya Energiya, 60, 141 (1986).
6. Maslov V.M. In: Proc. 5th Workshop on Neutron Measurements, Evaluations and applications. Nuclear Data for sustainable nuclear energy, JRC-IRMM-EU (Geel, Belgium), 27-29 October, 2008, Ljubljana, Slovenia, p. 73, 2008.
7. Maslov V.M., in: Proc. Intern. 2nd Intern. Conf. Frontiers in Nuclear Structure, Astro-physics and Reactions. FINUSTAR 2. Crete, Greece, 10-14 September 2007, AIP, CP-1012, 2008, p. 398.
8. Maslov V.M. Atomic Energy, 104, 4, 330 (2008).
9. Daroczy S., Raics P., Csikai J., Kornilov N.V. et al., Atomnaya Energiya, 58, 117 (1985).
10. Gromova E.A., Kovalenko S.S., Nemilov Yu.A. et al., Atomnaya Energiya, 54, 198 (1983).
11. Nishi T., Fujiwara I., Imanishi N., NEANDC(J_-42L, 20, 1975.
12. Landrum J.H., Nagel R.J., Lindner M., Phys. Rev. C 8, 1938 (1973).
13. Paulson C.K., Hennelly E.J., Nucl. Sci. Eng. 5, 24 (1974).
14. Lindeke K., Specht S., Born H.J., Phys. Rev. C 12, 1507 (1975).
15. Perkin J.L., Coleman R.F., Ann. Nucl. Energy, 14, 69 (1961).
16. Myers W.A., Lindner M., Newburry R.S., Journ. Inorg. Nucl. Chem. 37, 637 (1975).
17. Sood P.C. Z. Phys. A-Atomic Nuclei, 348, 111 (1984).
18. Lindner M., Dupzyk R.J., Hoff R.W. and Nagle R.J., J. Inorg. Nucl. Chem., 43, 3071 (1981).
19. Huizenga J.R., Vandenbosh R. Nuclear Fission, 1964, vol. 2, p. 51, Atomizdat.
20. Koning A.J., Rochman D., Sublet J. et al., Nuclear Data Sheets 155, 1 (2019); https://tendl. web.psi.ch/tendl_2021/tendl2021.html
21. Strutinsky V.M., Groshev L.V., Akimova M.K., Atomnaya Energiya, 38, 598 (1960).
22. Dovbenko A.G., Zakharova S.M., Kolesov V.E., Malyshev A.V., Atomnaya Energiya, 18, 114 (1964).
23. Uhl M., Strohmaier B., IRK-76/01, IRK, Vienna (1976).
24. Ahmad J. Hines J. and Cindler J.E., Phys. Rev. C27, 2239 (1983).

25. Gray P.H. Phys. Rev. 101, 306 (1956).
26. Cindler J. and Sjoblom R. J. Inorg. Nucl. Chem. 12, 8 (1959).
27. Lederer C.M., Jaklevic J.M. and Prussin S.G., Nucl. Phys., A135, (1969).
28. Gorman D.J., Asaro F., Phys. Rev. C, 2, 2406 (1970).
29. Maslov V.M., Porodzinskij Yu.V., JAERI Research, 98-038, 1998.
30. Shibata K., Iwamoto O., Nakagawa T. et al. J. Nucl. Sci. Technol., 48, 1 (2011).
31. Brown D., Chadwick M., Capote R. et al. Nuclear Data Sheets, 148, 1 (2018).
32. Maslov V. M., Porodzinskij Yu. V., Baba M. et al. IAEA-NDS-164. Vienna: IAEA, 2003, https://www-nds.iaea.org/minskact.
33. Firestone R.B., Table of Isotopes CD-ROM, Eighth Edition, Version 1.0, March 1996, S.Y. Frank Chu, CD-ROM Ed., V.S.Shirley, Ed., Wiley-Interscience, 1996
34. Browne E., Tuli J.K., Nuclear Data Sheets, 107, 2649 (2006).
35. Decay Radiation Data Base, version 12/11/2009, www.nndc.bnl.gov/ nudat2/index dec.jcp
36. Zolotarev K.I., INDC(NDS)-0546, IAEA, Vienna, April 2009.
37. Zolotarev K.I., Evaluation of cross-section data for the U-238(n,2n)U-237 reaction from threshold to 30 MeV. Private communication, Obninsk, FEI, May 2009.
38. Pronyaev V.G. et al., In: Proc. of Int. Conf. on Nuclear Data for Science and Technology, Santa Fe, New Mexico, USA, September 26 - October 1, 2004.
39. Maslov V.M., Physics of Particles and Nuclei Letters, 20, 565 (2023).
40. Maslov V.M., Physics of Particles and Nuclei Letters, 20, 1401 (2023).
41. Maslov V.M., Porodzinskij Yu. V., Baba M., Hasegawa A., Kornilov N. V., Kagalenko A. B., Tetereva N.A., Phys. Rev. C, 69, 034607 (2004).
42. Boykov G.S., Dmitriev V.D., Svirin M.I., Smirenkin G.N., Physics of Atomic Nucleus, 57, 2047 (1994).
43. Kornilov N.V., Kagalenko A.B., Baryba V.Ya. et al. In: Proc. of Intern. Conference on Nuclear Data for Science and Technology, May 19-24, Trieste, Italy, p.577.
44. Taieb J., Granier T., Ethvignot T. et al. In Proc. of the Inter. Conf. on Nuclear Data for Science and Technology (O. Bersillon, F. Gunsing, E. Bauge, R. Jacqmin and S. Leray, eds.), p. 429, Nice, France, April 22-27, 2007, EDP Sciences.
45. Trufanov A.M., Lovchikova G.N., Sukhih S.E. et al., Phys.Atom. Nucl., 55, 289(1992).
46. Than Win, Baba M., Ibaraki M. et al., J. Nucl. Sci. Techn. 36, 486 (1999).
47. Maslov V.M., Porodzinskij Yu. V., Tetereva N.A, Baba M., Hasegawa A. Nucl. Phys. A 736, 77 (2004).
48. Kovalenko S.S., Selitsky Yu.A., Funshtein V.B., Khlebnikov S.V., Yakovlev V.A., Proc. Int. Conf. Nuclear Data for Science and Technology, Mito, USA, September 6-10, 1988, p. 995, 1988.
49. Aaltonen J., Brenner M., Egorov S.A., et al., Phys. Rev. C, 41,513 (1990).
50. Turkevich A., Radiochimica Acta, 64, 145 (1994).
51. Guzhovskii B.Ya., Abramovich S.N., Zvenigorodskii A.G. et al., Proc. Int. Conf. Nuclear Data for Science and Technology, Gattlinburg, USA, May, 1994, p. 390,1994.
52. Bellido L.F., Robinson V.J., Sims H.E., Radiochimica Acta, 64, 11 (1994).
53. Uosif M.A.M., Michel R., Herpers U., et al. In: Proc. Int. Conf. Nuclear Data for Science and Technology, Santa Fe, USA, October, 2004, p. 1547, 2005.
54. Ageev A., Golovnya V.Ya., E.A.Gromova et al., Yad. Fyz., 46, 700 (1987).
55. McCormick G.H., Cohen B.L., Phys. Rev. 96, 722, (1954).
56. Yokoyama A., Takahashi N., Nitani N. et al., Zeit. Phyz./A, 356, 55 (1996).

57. Zhao Y.L., Tanikawa M., Sueki K., et al., Radiochimica Acta, 86, 79 (1999).
58. Boyce J.R., Hayward T.D., Bass R. et al., Phys. Rev. C 10, 231(1974).
59. Kandil A.T., Journ. Inorg. Chemistry 38, 37 (1976).
60. Fulmer C.B., Phys. Rev. 116, 418 (1959).
61. Isaev S., Prieels R., Keutgen Th. et al. Nucl. Phys. A 809, 1 (2008).
62. Baba S., Umezawa H., Baba H., Nucl. Phys. A 175, 177 (1971).
63. Maslov V.M., Phys. Lett. B, 649, 863 (2007).
64. Maslov V.M., Yad. Fyz., 86, 562 (2023).